Influence of experimental procedure on d-spacing measurement by XRD of montmorillonite clay pastes containing PCE-based superplasticizer

Pere Borralleras[a], Ignacio Segura[b, c,*], Miguel A. G. Aranda[d] and Antonio Aguado[b]

[a] BASF Construction Chemicals Iberia, Ctra del Mig 219, E-08907 Hospitalet de Llobregat, Barcelona, Spain

[b] Department of Environmental and Civil Engineering, Universitat Politècnica de Catalunya-Barcelona Tech, Jordi Girona 1-3, C1, E-08034 Barcelona, Spain

[c] Smart Engineering Ltd, Jordi Girona 1-3, ParcUPC–K2M, E-08034 Barcelona, Spain

[d] ALBA Synchrotron, Carrer de la Llum 2-26, E-08290, Cerdanyola del Vallès, Barcelona, Spain

* Corresponding author: Ignacio Segura, Department of Environmental and Civil Engineering, Universitat Politècnica de Catalunya-Barcelona Tech, Jordi Girona 1-3, C1, E-08034 Barcelona, Spain. Email address: ignacio.segura@upc.edu Tel: +34 93 4054684

Abstract

This study investigates the influence of the experimental procedure on determining the d-space enlargement of montmorillonite clay (MNT) produced by the absorption of polycarboxylate (PCE) based superplasticizers. d-spacing alterations registered by in situ X-ray Diffraction (XRD) analysis on fresh clay pastes have been compared against the results obtained when clay pastes are previously centrifuged and dried (reference methodology reported in bibliography). Data from experiments show

relevant differences between the two methodologies. While MNT clay d-spacing present limited expansion when recorded on samples previously separated and dried, direct XRD for fresh clay pastes shows much larger expansion of inter-laminar space. Clay expansion evolves with the increase of PCE dosage up to 3 times larger than typical data recorded when samples previously dried. The results shown here indicates that information collected following the typical experimental procedure based on sample drying could not be representative of MNT clay interference on dispersion mechanism of PCE superplasticizers.

Keywords: XRD (C), Polycarboxylate (E), Clay (C), d-spacing (E), Portland cement (B), Intercalation (D)

1. Introduction

The capacity of montmorillonite clays (MNT) to inhibit the dispersing capacity of PCE-based superplasticizers for concrete is well known [1]. The interference mechanism is based on the preferential intercalation of polyethylene oxide/polyethylene glycol (PEO/PEG) side-chains of the PCE polymer in the MNT interlaminar space. From an initial d-spacing of 12.3–12.6 Å or 15.0–15.5 Å (depending on the degree of clay hydration) when no admixture is present [2, 3], PCE intercalation produces a d-spacing expansion of up to 17–18 Å when a PCE-based superplasticizer is used. This enlargement has been reported to correspond to one single intercalated poly-glycol chain in MNT clay, coordinated with water molecules [4-8]. All available studies in the literature address the interaction of clays with PCE-based superplasticizers via the same experimental procedure [1,4,8]. PCE-clay pastes are centrifuged and the solid residue is extracted. Subsequently, this residue is dried at temperatures between 40–80 ºC in all cases.

Other studies [8,9] have reported similar MNT d-spacing expansions by following the same experimental process, as shown in Fig 1. Nevertheless, other authors [10] reported experiments where the observed d-spacing expansions of MNT clays were not homogeneous and varied depending on the structure of the PCE polymer and the nature of MNT clay. In general, they reported expansions in the range of 4.9–5.5 Å.

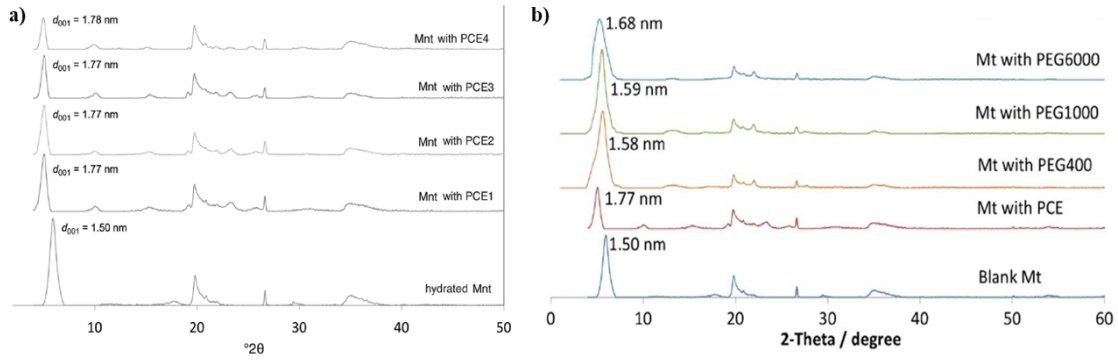

Fig. 1. a) Laboratory XRD patterns for centrifuge-dried MNT samples with different PCE-based superplasticizers (adapted from [5]); b) Laboratory XRD patterns for centrifuge-dried MNT samples with PCE- and PEG-based superplasticizers (adapted from [9])

The main objective of our study is to identify the influence of the sample preparation procedure on the d-spacing expansion of clay-PCE pastes as measured by XRD techniques, since clay interference with PCE superplasticizer dispersion capacity is an exclusive effect of fresh state systems. Moreover, superplasticizer admixtures that can be more resilient to the negative effect of clay in aggregates have been very recently highlighted as a research priority [11], and can only be attained with a well-established, robust, methodology.

In this investigation, XRD patterns were recorded directly from fresh pastes of MNT clay, including different dosages of a PCE-based admixture without any phase separation or drying process. To provide a frame of comparison, clay pastes having identical composition were prepared according to the standard procedure described in the literature [1] and powder XRD patterns were recorded. To extend the assessment of the influence of the experimental methodology on the final clay d-spacing and to confirm the reproducibility of the results obtained when testing fresh samples directly*, in situ* XRD measurements were performed with two different X-ray diffractometers at two different facilities: standard laboratory XRD (Cu X-ray tube) and X-ray synchrotron radiation analyses. It should be noted that synchrotron radiation techniques are especially suited for carrying out *in situ* studies on unaltered cement pastes [12]

2. Materials

The materials used for the preparation of pastes were sodium montmorillonite powder and pure non-formulated PCE polymer. The liquid phase used to produce the pastes was always a synthetic cement pore solution as a simulant of the liquid phase formed during the early-age hydration of Portland cement.

2.1 Sodium montmorillonite clay (Na-MNT)

The clay sample used was a sodium montmorillonite (Na-MNT) clay powder. Oxide composition by XRF is shown in Table 1, expressed in oxide wt.%. Measured BET specific surface was 49.5 m^2/g (average of two measurements: 46.1 m^2/g and 52.8 m^2/g). The crystalline composition of Na-MNT clay was obtained by laboratory powder XRD analysis (see Fig 2). The clay presents basal displacement d_{001} of 12.3 Å deduced from

its 2θ position at 7.2º. This value is typical for Na-MNT clays with one H_2O molecule layer inside the interlaminar space [3] [11]. 4.8 wt.% of quartz and 3.3 wt.% of calcite were identified as minor impurities, so the last explains the LOI value observed. Both quartz and calcite impurities cannot intercalate polycarboxylate side chains thus not influencing in the interpretation of the experimental results [9].

SiO_2	TiO_2	Al_2O_3	Fe_2O_3	MgO	MnO	TiO	CaO	K_2O	Na_2O	LOI	Total
63.12	0.01	19.88	1.37	2.33	0.04	0.06	2.24	0.44	3.43	5.97	98.89

Table 1. Oxide composition in wt.% by XRF for Na-MNT clay sample

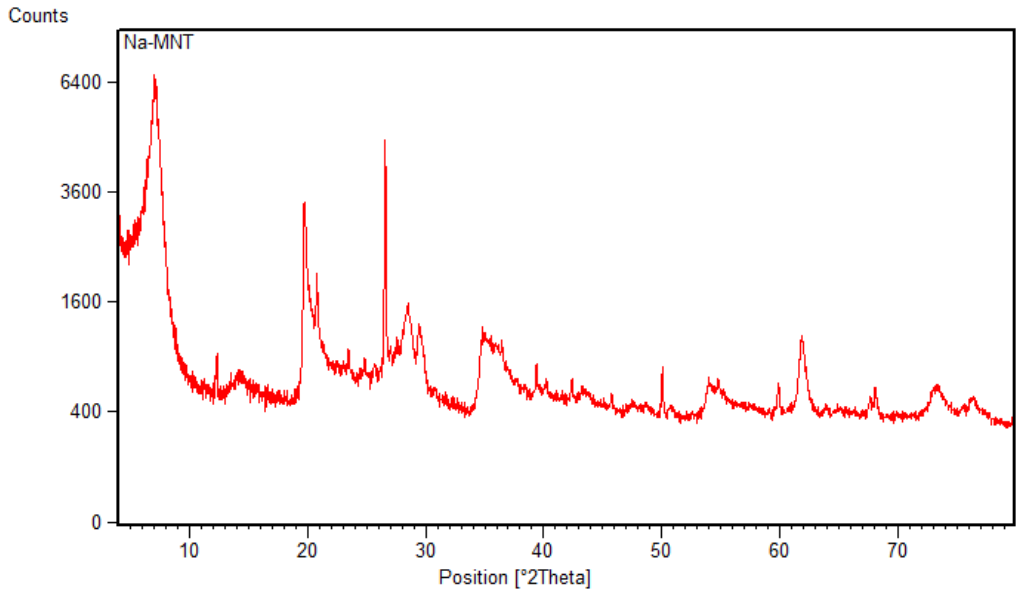

Fig. 2. Laboratory XRD pattern for raw Na-MNT used in this study.

2.2 Polycarboxylate superplasticizer

Pure PCE polymer based on poly(ethylene glycol) ether on polyacrylate backbone from BASF Construction Chemicals was used. It is available in water-solution at 51 wt. % concentration. Basic PCE characteristics are given in Table 2. Dosages of the PCE

admixture are always referred to percentage of PCE active solids by weight of clay (expressed as % bwc).

Parameter	Value
Side-chain length	1.100 g/mol (25 mol EO)
Total carboxylic (by titration)	95 mg KOH/g PCE
Polymer type	PEG side chain on acrylic backbone

Table 2. Chemical structure and characterization of PCE polymer

2.3 Synthetic cement pore solution

All clay pastes were produced using synthetic cement pore solution as the liquid phase. This solution is prepared by dissolving 14.3 g of Na_2SO_4, 3.05 g of NaOH and 3.00 g of $Ca(OH)_2$ in 1 litre of distilled freshly-boiled water (equivalent to 0.157 mol/l of OH^-, 0.278 mol/l of Na^+, 0.100 mol/l of SO_4^{2-} and 0.040 mol/l of Ca^{2+} concentration). Synthetic cement pore solution used here was always recently prepared to avoid minimise carbonation.

3. Experimental methods

3.1. Preparation of clay pastes

Mixing procedures are reported to affect the admixtures' performances [13]. Therefore, the same mixing procedure is always carried out here. Clay pastes were prepared at 22 ºC by dispersing 10 g of powder clay in 50 g of synthetic cement pore solution to produce a 16.7 wt. % paste concentration. The mixing process was done with a vertical shaft mixer equipped with a helical head, at 1200 rpm. The total mixing time was three minutes. The admixture was incorporated at the required dosage at the one-minute mixing time.

3.2 *In situ* XRD of fresh clay pastes with synchrotron X-ray source

XRD patterns for six clay pastes were performed, including the reference paste at 16.7 wt. % concentration without the admixture and pastes with 13%, 50%, 100%, 220% and 325% bwc active solids of PCE polymer. Each fresh clay paste was introduced into a thin glass capillary of 1.5 mm diameter just after mixing. Capillaries filled with fresh clay pastes were mounted on a capillary rack, as shown in Fig. 3.

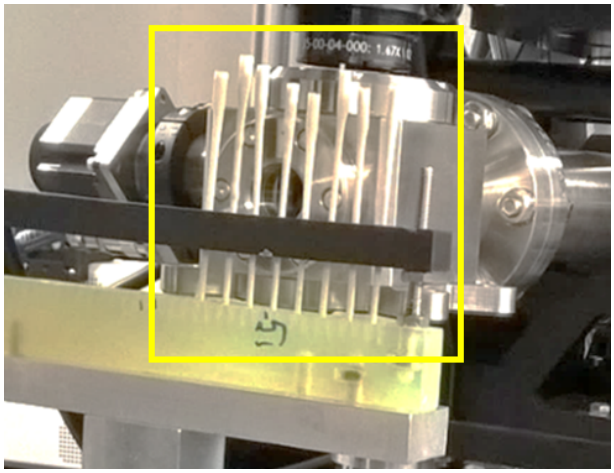

Fig. 3. Capillaries containing the fresh pastes mounted on the rack for synchrotron XRD data collection.

Samples were measured on the BL11-NCD device of ALBA Synchrotron (Barcelona). Small angle X-ray scattering (SAXS) and wide angle X-ray scattering (WAXS) patterns were simultaneously recorded at 12.4 keV. The sample detector distances were 2.450 m and 0.170 m for SAXS and WAXS respectively. The WAXS detector was tilted by 27° along the horizontal axis perpendicular to the beam path. The beam stop was located on the top left corner of the SAXS detector and the data acquisition time was five seconds.

3.3 *In situ* XRD patterns of fresh pastes with standard Cu Kα lab diffractometer

XRD patterns for clay pastes without the admixture and clay pastes including different dosages of PCE were recorded at the CCiT facilities of the University of Barcelona using a laboratory X-ray powder diffractometer. Fresh pastes were sandwiched between two polyester films (thickness of 3.6 μm) and locked by two metallic rings as shown in Fig. 4.

Fig. 4. Holder containing the fresh pastes, sandwiched between thin polyester films, for Cu Kα laboratory XRD data collection.

A PANalytical X'Pert PRO MPD diffractometer of 240 mm of radius was used, in a configuration of convergent beam with a focalizing mirror and a transmission geometry with flat samples sandwiched between low absorbing films. Cu Kα radiation (λ = 1.5418 Å) was produced by an X-ray tube operating at 45 kV–40 mA and measured by a PIXcel detector with active length = 3.347 º. The incident beam slits defining a beam height were 0.4 mm for wide-angle and 0.05 mm for small-angle. Two 2θ/θ scans were recorded: i) SAXS data from 0.3 to 12 º2θ with a step size of 0.013 º2θ and a measuring

time of 647 seconds per step; and ii) WAXS data from 2 to 30 º2θ with a step size of 0.026 º2θ and a measuring time of 148 seconds per step.

3.4 Powder XRD patterns of separated-dried clay pastes

Clay pastes were also prepared following the same mixing process and transferred into a centrifuge tube. Samples were centrifuged at 10,000 rpm for 12 minutes. As an alternative approach to the centrifugation method for phase separation, some clay pastes were separated by filtration using a Buchner funnel powered by suction. The solids were collected, washed and dried at 40 ºC for seven days. Subsequently, the solid deposits were collected and dried at 40 ºC for seven days. Powder XRD patterns of the dried solid fractions were collected by using the same PANalytical X'Pert PRO MPD Cu Kα laboratory diffractometer at the CCiT facilities of the University of Barcelona. The incident beam slits defining a beam height were 0.4 mm for wide-angle and 0.05 mm for small-angle. The 2θ/θ scan conditions were: i) SAXS data from 0.2 to 6 º2θ with a step size of 0.013 º2θ and a measuring time of 800 seconds per step; ii) WAXS data from 2 to 60 º2θ with a step size of 0.026 º2θ and a measuring time of 298 seconds per step.

4. Results and discussion

4.1 Influence of separation method on d-spacing of dried clay pastes

Prior to evaluating the possible impact of sample drying process on d-spacing measurement, the influence of separation method on XRD results of dried clay pastes was investigated. XRD patterns collected from dried clay pastes containing 13% bwc of PCE are shown in Fig. 5, where it is compared with the patterns for the samples separated using both centrifugation and filtration methods.

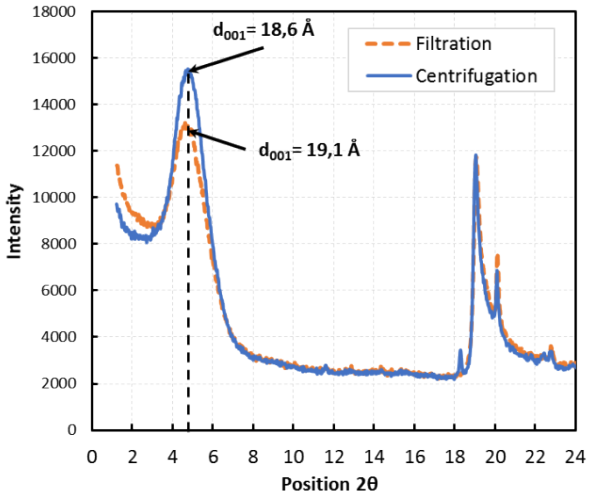

Fig. 5. Laboratory XRD patterns for dried clay pastes by using two different separation methods.

From Fig. 5, it can be stated that both clay d-spacing results of 18.6 Å and 19.1 Å do not differ significantly from the literature values, using the same sample preparation approaches [3-5]. The difference in d-spacing observed in Fig. 5 between centrifugation and filtration separation methods (≈ 0.5 Å) is not very significant. Thus, it can be deduced that separation method has a minor influence on d-spacing measurements on dried clay pastes.

4.2 Influence of clay paste drying process on d-spacing measurements

Figure 6 displays the XRD patterns obtained with the non-separated, non-dried fresh clay paste series, as prepared without the admixture, with 13% bwc and with 50% bwc of PCE polymer. Synchrotron XRD patterns from fresh pastes collected at ALBA and laboratory XRD data are shown in Fig. 6(a) and Fig. 6(b) respectively. For the sake of comparison, Fig. 6(c) displays the laboratory XRD patterns for the same samples but after centrifugation and drying processes.

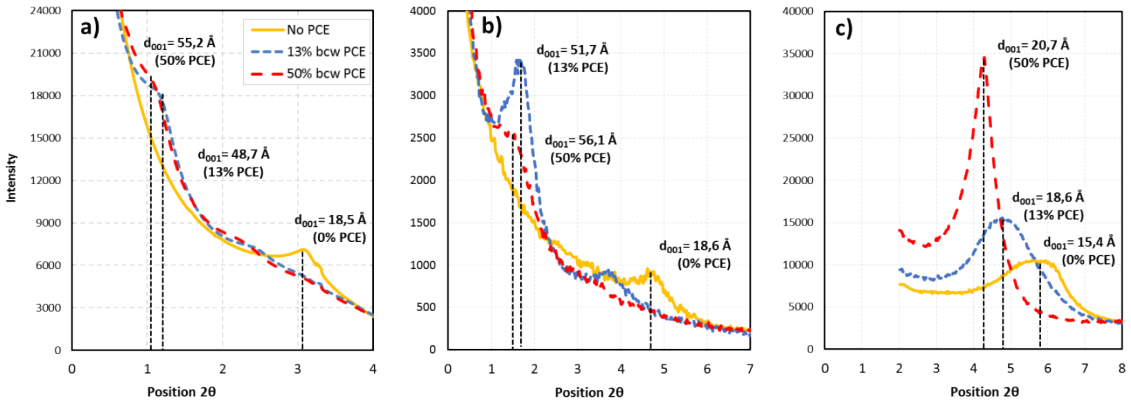

Fig. 6. XRD patterns for Na-MNT pastes with increasing PCE content for: a) fresh pastes collected with synchrotron radiation; b) fresh pastes collected with a Cu Kα diffractometer; c) centrifuged and dried pastes collected with a Cu Kα diffractometer.

The d_{001} spacing obtained from the XRD patterns shown in Fig. 6 are listed in Table 3. This value provides the basal spacing or layer stacking in a phyllosilicate. Despite using different equipment, the values presented in Table 3 are similar for the *in situ* analyses of fresh pastes at the three tested dosages. Conversely, the basal spacing obtained from powder XRD analyses are undeniably much lower at all PCE dosages. For clay pastes containing PCE polymer, the basal spacing measured from powder XRD analyses are compatible with d-spacing's observed in MNT clay pastes with a single intercalated monolayer of PEO/PEG side-chains [16]. These experimental results are in agreement with values obtained under similar conditions by other authors [4, 5, 7, 9, 10].

Sample	d_{001} spacing (Å)		
	In situ XRD (fresh paste)		Powder XRD (dried paste)
	Synchrotron	Cu Kα	Cu Kα
0% PCE	18.5	18.6	15.4
13% PCE	48.7	51.7	18.6
50% PCE	55.2	56.1	20.7

Table 3. Basal spacing (d_{001}) obtained from XRD measurements of clay-PCE pastes

231

232 Chiefly, when comparing *in situ* XRD patterns of fresh pastes with powder XRD
233 patterns of dried pastes, major differences in d-spacing values are observed. This direct
234 experimental result clearly indicates that some intercalated PCE side-chains and water
235 molecules are lost during the drying process, thereby causing a reduction in the measured
236 expansion. Therefore, we are forced to conclude that the final d-spacing recorded is
237 critical on sample treatment by drying and it can be misleading as correlations should be
238 established in the fresh paste state.

239

240 XRD measurements for clay-PCE dried samples suggest intercalation of one
241 single monolayer of PEG/PEO side-chains with two water molecules. However, *in situ*
242 XRD data for similar samples but recorded in fresh pastes could be indicative of a
243 mechanism based on multiple intercalated layers of side-chains. To the best of our
244 knowledge, there are no references reporting diffraction data in these experimental
245 conditions. Therefore, more studies by independent laboratories are needed to firmly
246 establish this behaviour.

247

248 d_{001} d-spacing values corresponding to fresh clay pastes without admixture (see
249 Table 3), are compatible with MNT clay with three water molecules in the interlayer
250 region, typical in calcium alkaline media [2, 3]. When clay pastes without admixture are
251 dried, the original d_{001} spacing of 12.3 Å of raw-powder clay increases to 15.4 Å. This
252 basal spacing value is referred to in publications as characteristic of calcium
253 montmorillonite with two water molecules in the interlayer region [2, 3, 5]. This
254 observation indicates that not all absorbed water is lost during the drying process (even
255 considering that the tested sample was dried for 7 days at 40 ºC). The results also suggest

256 that some cation exchange could take place, sodium by calcium, while the clay is
257 dispersed in the cement pore solution.
258
259 **4.3 Impact of PCE dosage on Na-MNT d-spacing expansion**
260 To further investigate the influence of PCE dosage on the expansion of Na-MNT
261 interlaminar space, an additional XRD study was performed. Fig. 7 reports the d-spacing
262 values, obtained from synchrotron and laboratory XRD patterns, for clay pastes prepared
263 with increasing dosage of PCE admixture.
264

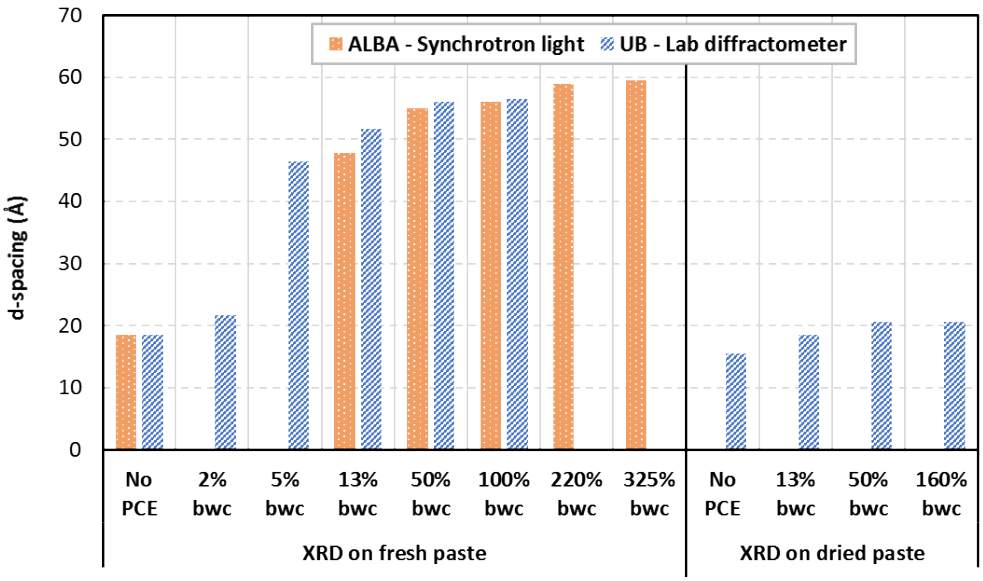

265
266 Fig. 7. d-spacing of clay pastes with different PCE dosages and different XRD
267 diffraction measurement conditions
268
269 Firstly, laboratory XRD data for corresponding dried samples show much smaller
270 d-spacing values as shown in Fig. 7. Secondly, d-spacing variations recorded in dried clay
271 pastes containing PCE from 13% bwc to 160% bwc show no significant difference.
272 Maximum d-spacing of 20.7 Å is observed at PCE dosage of 50% bwc, which is identical,
273 within the errors, to that of 160% bwc. For all dried samples, the obtained results are

compatible with one single monolayer of intercalated PEO/PEG side-chain in a zig-zag planar disposition coordinated by two water molecules [7, 10]. Thirdly, for the fresh paste samples, changes in d-spacing values are observed with increasing PCE dosage, with both diffraction equipment set-ups.

The largest observed d-spacing is close to 60 Å, being three times the maximum value obtained for dried clay pastes. From this observation, it can again be concluded that dried pastes do not reproduce the real impact on interlaminar expansion generated by PCE dosages, as observed in XRD patterns for fresh clay pastes (see Fig. 7). The large d-spacings (layer expansion) observed upon PCE intercalation has been assigned to regular side chains intercalation between the clay layers. At this stage, it is not possible to rule out irregular side chain intercalation each few clay layers. This will be studied in a future research, but it does not affect the main findings of this work: the previously reported sample preparation for XRD yielded misleading results. Finally, d-spacing expansions recorded on fresh pastes by using synchrotron and laboratory XRD sources are quite similar for all PCE tested dosages. Therefore, we infer that the experimental conditions used for the diffraction experiments do not affect the results.

5. Hypothesis for PCE intercalation model in MNT clay

Based on the observed d-spacing expansion, a hypothesis for the PCE intercalation model on MNT clay can be proposed. The theoretical thickness of one monolayer of water molecules within the interlaminar space can be estimated by assuming a thickness of 9.6 Å for the T-O-T layer structure of MNT clay [17]. Thus, inter-layer space can be deduced by subtracting this value from the experimental d-spacing values. Table 4 presents some reported d-spacing data from various references as well as from proposed coordination

299 models, which allows for the derivation of the theoretical H_2O monolayer thickness. As
300 can be seen, almost all values are between 2.7 Å and 2.9 Å. The resulting average value
301 of 2.81 Å would correspond to the thickness of one single H_2O monolayer within the
302 MNT interlaminar space. This result is in agreement with hydrogen bonding lengths in
303 similar structures [19].
304

Data source		Sample state	d-spacing (Å)	Coord. H_2O layers	Calc. length of H_2O monolayer (Å)
[18]		dried	12.6	1	3.0
[4]			12.3	1	2.7
[3]		fresh	19.1	3	3.17
[10]		dried	15.2	2	2.8
[2]		simulation	12.3–21.0	1–4	2.7–2.85
[5]		dried	15.0	2	2.7
This study	Cu Kα	Raw	12.3	1	2.7
		dried	15.4	2	2.9
		fresh	18.6	3	2.99
	Synchrotron		18.5	3	2.97

305 Table 4. d-spacing data for MNT clay without PCE admixture
306

307 To theoretically estimate the thickness of one single PEG/PEO side-chain,
308 intercalated into the MNT interlaminar space, Table 5 presents d-spacing results from
309 references for MNT pastes treated with PCE polymers. Assuming an intercalation model
310 where PEG/PEO side-chain is coordinated with two water molecules by hydrogen
311 bonding [9], and arranged in a zig-zag planar disposition [7], the equivalent thickness of
312 one single PEO monolayer can be deduced from the proposed configuration, as presented
313 in Table 5. The result of the simple calculation is 2.48 Å. Considering a thickness of 2.81
314 Å for H_2O monolayer and 2.48 Å thickness for PEG/PEO side-chain monolayer and by
315 accepting the intercalation model proposed, it is possible to calculate the number of H_2O
316 and PEO unit layers intercalated in fresh clay pastes. The number of intercalated layers

317 calculated from d-spacing results obtained from synchrotron XRD source are given in
318 Table 6.
319

Reference	Sample state	d-spacing (Å)	H_2O:PEO coordination	Calculated length of PEO monolayer (Å)
[4]	dried	17.7	2:1	2.3
[5, 7, 9]	dried	17.8 17.7	2:1	2.4 2.3
[20]	simulation	17.9	2:1	2.5
[1, 8]	dried	17.2	2:1	2.0
[10]	dried	17.6 17.8 17.9	2:1	2.2 2.4 2.5

320 Table 5. d-spacing data for MNT clay with PCE admixture
321

PCE dosage (% bwc)	d-spacing (Å)	H_2O layers coordinated	PEO layers coordinated	Error (Å)
13%	48.7	8	7	-0.7
50%	55.2	9	8	0.5
100%	56.1	9	8	1.4
220%	58.9	10	9	-1.1
325%	59.5	10	9	-0.5

322 Table 6. Calculated H_2O and PEO layers intercalated into MNT clay
323

324 By comparing intercalated units of PEG/PEO side-chains from XRD patterns of
325 fresh clay pastes (Table 6) with intercalation number deduced from XRD patterns of dried
326 clay pastes (Table 5), it is possible to conclude that the degree of intercalation of PCE
327 side-chains is up to nine times larger and increases with PCE dosage. The error calculated
328 as the difference between theoretical (simplified) calculations and experimental d-spacing
329 are also reported in Table 6. The maximum observed error, 1.4 Å, can be considered low
330 and within the errors and approximations. Therefore, it would be possible to validate the
331 model of multiple intercalation based on PEG/PEO side-chains coordinated with H_2O

molecules by H-bonding. This means that the theoretical thickness deducted for one H_2O-PEO layer corresponds to 5.3 Å, which fits with most reported data [1, 7, 10] while being in agreement with the experimental results reported here.

A scheme of the multiple intercalation model is displayed in Fig. 8(b), derived from an initial configuration of three H_2O layers where no PCE admixture is present, as shown in Fig. 8(a). When PCE polymer is added, Fig. 8(b) proposes an intercalation model based on repetitive sequences of H_2O-PEO layers ($L_{H_2O\text{-}PEO}$) ended by a single H_2O monolayer bonded to internal MNT clay surface by H-bonding.

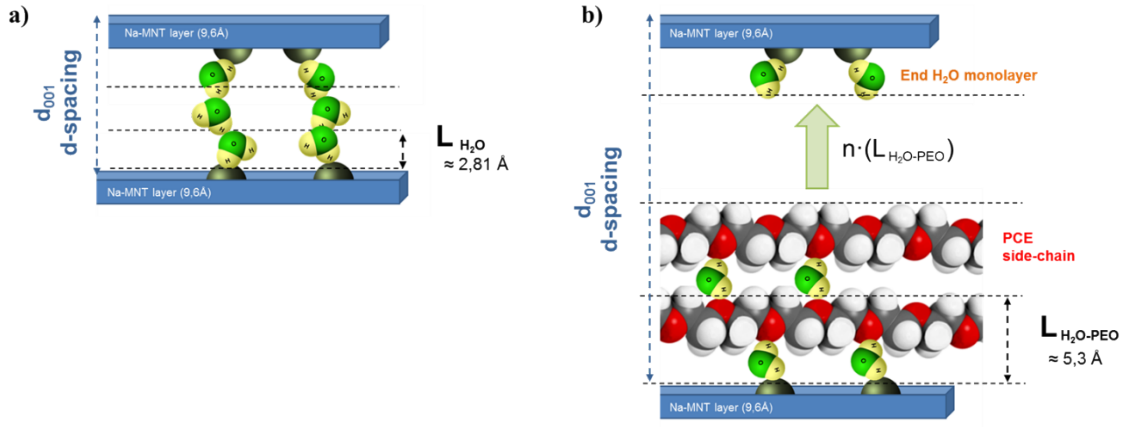

Fig. 8. Intercalation models in MNT clay; a) without PCE polymer added; b) with PCE based admixture added

In situ XRD data from fresh clay pastes indicate that up to nine PEG/PEO side-chains of PCE polymer can be intercalated in a single interlaminar space of MNT clay. This value is much larger than the intercalation numbers deduced from powder XRD patterns for dried clay samples. Considering the potential steric repulsion derived from the concentration of a large number of long PEG/PEO side-chains in a limited space, it is possible to propose that all side-chains intercalated in a single unit of dispersed MNT

clay particle belongs to a restricted number of polymer units or even to a unique PCE molecule adsorbed on the clay surface. The multiple intercalation model proposed is not in contradiction with the mechanisms proposed by Ng & Plank [4] Tan et al. [7]. In fact, the assumed molecular interaction is the same as that proposed by the aforementioned authors, but data from *in situ* XRD patterns obtained on fresh clay pastes allow for an extension of the initial PEG/PEO monolayer model of intercalation to a multiple-chain intercalation model, where many PCE side-chains can be absorbed at the same time into interlaminar space of MNT clay.

6. Conclusions

An undesired influence of the drying process of clay pastes on d-spacing determination by XRD has been identified. Changes in d-spacing due to the intercalation of PCE side-chains measured in dried clay pastes by powder XRD are systematically much lower than the changes observed by *in situ* XRD recorded for fresh pastes. Absolute d-spacing values, when the PCE admixture is used, are altered by the drying process, and up to nine times lower number of intercalated PEG/PEO side-chains are observed. Furthermore, the dried sample XRD data does not reproduce the true degree of intercalation as the dosage of PCE admixture increases.

The behaviour of fresh paste analysis has been confirmed by performing *in situ* measurements with two different sets of equipment, a synchrotron and a laboratory diffractometer, which yielded comparable results. Based on these observations, a multiple intercalation model of PCE side-chains has been proposed, based on a sequence of overlapping H_2O-PEO layers ending with a H_2O monolayer.

Acknowledgments

Mr. Borralleras is grateful for all the support given by BASF Construction Chemicals to the development of this work. Dr. I. Segura is supported by the postdoctoral Torres Quevedo program of the Spanish Ministry of Economy and Competitiveness.

References

[1] L. Lei, J. Plank, A concept for a polycarboxylate superplasticizer possessing enhanced clay tolerance, Cement and Concrete Research 42 (2012) 1299-1306.

[2] S. Karaborni, B. Smit, W. Heidug, J. Urai. E. van Oort, The swelling clays: molecular simulations of the hydration of montmorillonite, Science 271 (1996) 1102-1104.

[3] M. Matusewicz, K. Pirkkalainen, J.P. Suuronen, A. Root, A. Muurinen, R. Serimaa, M. Olin, Microstructural investigation of calcium montmorillonite, Clay Minerals 48 (2013) 267-276.

[4] S. Ng, J. Plank, Interaction mechanisms between Na-montmorillonite clay and MPEG-based polycarboxylate superplasticizers, Cement and Concrete Research 42 (2012) 847-854.

[5] H. Tan, Xin Li, M. Liu, B. Ma, B. Gu, X. Li, Tolerance of cement for clay minerals: effect of side-chain density in polyethylene oxide (PEO) superplasticizers additives, Clay and Clay Minerals 64-6 (2016) 732-742

[6] G. Xing, W. Wang, G. Fang, Cement dispersion performance of superplasticizers in the presence of clay and interaction between superplasticizers and clay, Advances in Cement Research 29 (2017) 194-205.

[7] H. Tan, B. Gu, B. Ma, X. Li, C. Lin, Mechanism of intercalation of polycarboxylate superplasticizer into montmorillonite, Applied Clay Science 129 (2016) 40-46.

[8] L. Lei, J. Plank, A study on the impact of different clay minerals on the dispersing force of conventional and modified vinyl ether based polycarboxylate superplasticizers, Cement and Concrete Research 60 (2014) 1-10.

[9] H. Tan, B. Gu, S. Jian, B. Ma, Y. Guo, Z. Zhi, Improvement of polyethylene glycol in compatibility with polycarboxylate superplasticizer and poor-quality aggregates containing montmorillonite, Journal of Materials in Civil Eng. 29-9 (2017).

[10] R. Ait-Akbour, P. Boustingorry, F. Leroux, F. Leising, C. Taviot-Guého, Adsorption of polycarboxylate poly(ethylene glycol) (PCP) esters on montmorillonite (MNT): Effect of exchangeable cations (Na^+, Mg^{2+} and Ca^{2+}) and PCP molecular structure, Journal of Colloid and Interface Science 437 (2015) 227-234.

[11] J. Cheung, L. Roberts, J. Liu, Admixtures and sustainability, Cement and Concrete Research, *in press*.

[12] M.A.G. Aranda, Recent studies of cements and concretes by synchrotron radiation crystallographic and cognate methods, Crystallography Reviews 22 (2016), 150-196.

[13] F. Winnefeld, Influence of cement ageing and addition time on the performance of superplasticizers, ZKG International 61 (2008), 68–77,

[14] G. Xing, W. Wang, G. Feng, Cement dispersion performance of superplasticizers in the presence of clay and interaction between superplasticizer and clay, Advances in Cement Research 29 (2017) 194-205.

425 [15] G. Xing, W. Wang, J. Xu, Grafting tertiary amine groups into the molecular
426 structures of polycarboxylate superplasticizers lowers their clay sensitivity, The Royal
427 Society of Chemistry, RSC Advances 6 (2016) 106921-106927.
428 [16] R.L. Parfitt, D.J. Greenland, The adsorption of poly(ethylene glycols) on clay
429 minerals, Clay Minerals 8 (1970) 305.
430 [17] R.A. Schoonheydt, C.Y. Johnston, The surface properties of clay minerals, EMU
431 Notes in Mineralogy 11-10 (2011) 337-373.
432 [18] D. Senich, T. Demirel, R.L. Handy, X-Ray diffraction and adsorption isotherm
433 studies of the calcium montmorillonite-H_2O system, Highway Research Record 209,
434 46^{th} Annual meeting of Physico-Chemical Phenomena in Soils (1956) 23-54.
435 [19] P.F. Low, J.L. White, Hydrogen bonding and polywater in clay-water systems,
436 Clays and Clay Minerals 18 (1970) 63-66.
437 [20] M. Szczerba, Z. Klapyta, A. Kalinichez, Ethylene glycol intercalation in
438 smectites. Molecular dynamics simulation studies, Applied Clay Science 91 (2014) 87-
439 97.
440

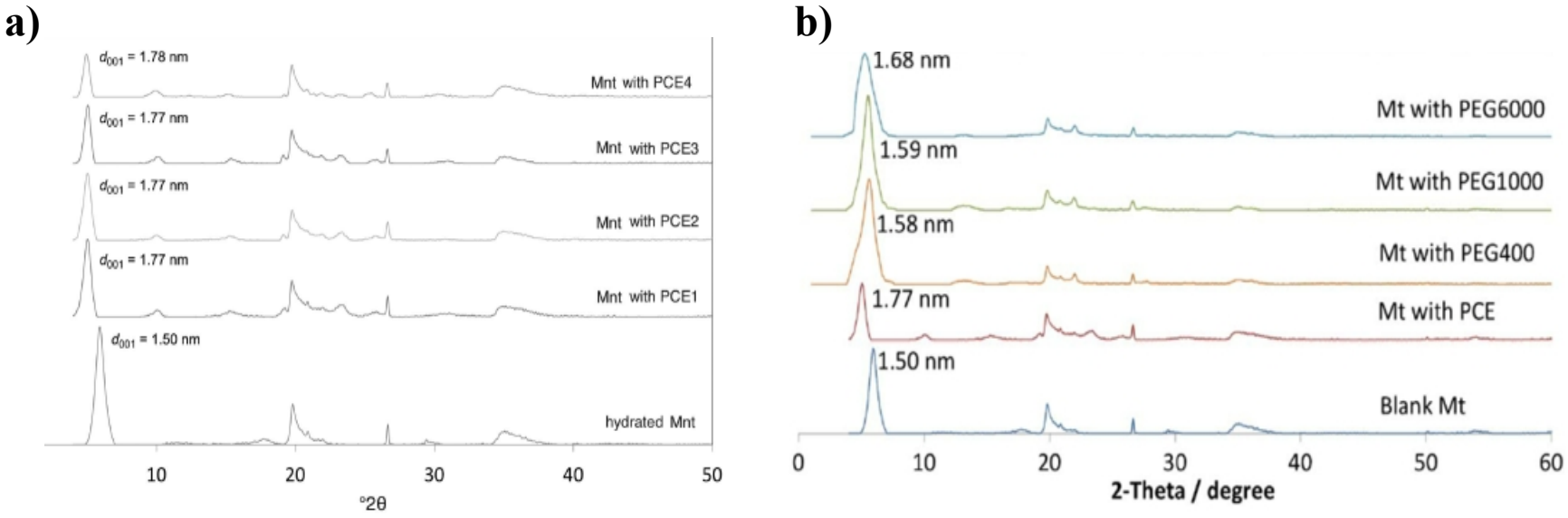

Fig. 1. a) Laboratory XRD patterns for centrifuged-dried MNT samples with different PCE based superplasticisers (adapted from [5]); b) Laboratory XRD patterns for centrifuged-dried MNT samples with PCE and PEG based superplasticisers (adapted from [9])

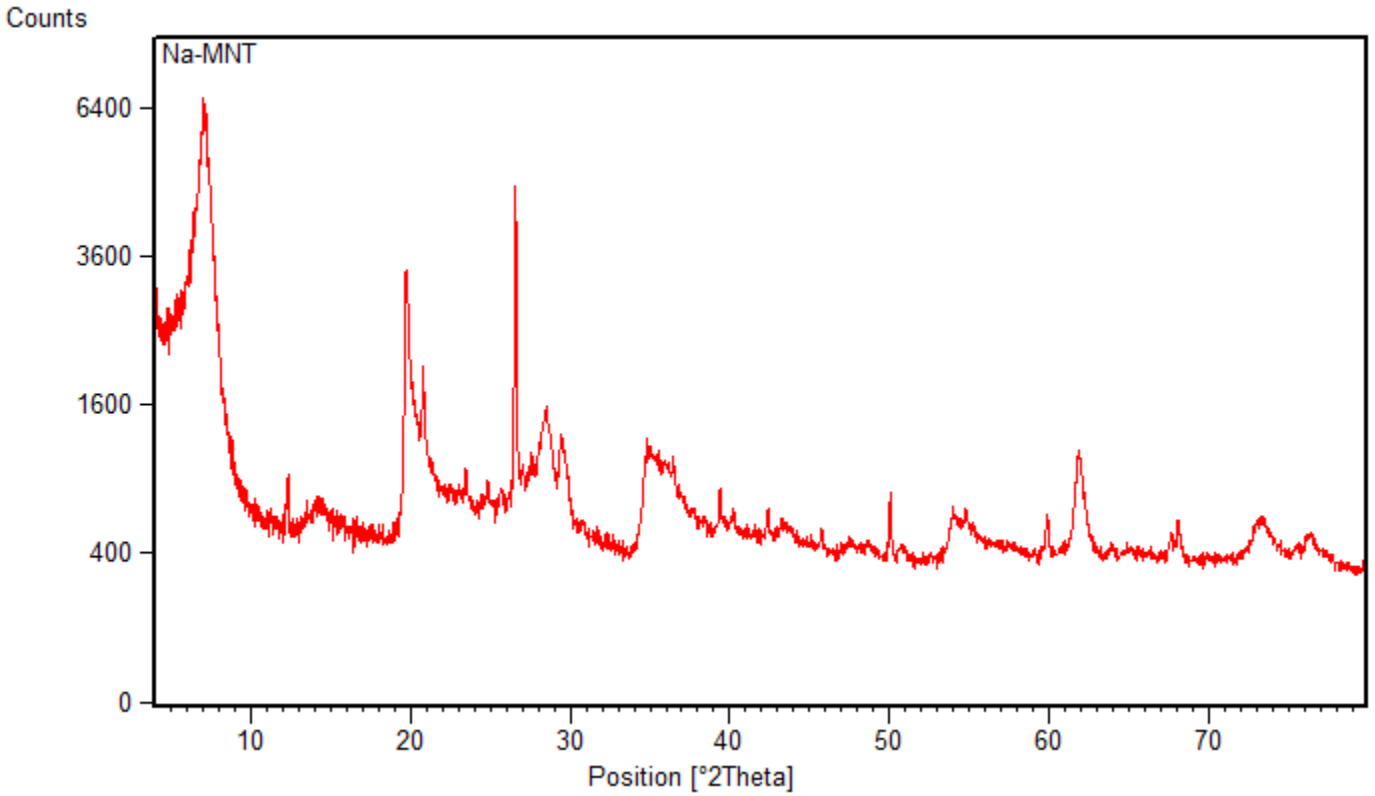

Fig. 2. Laboratory XRD pattern for raw Na-MNT used in this study.

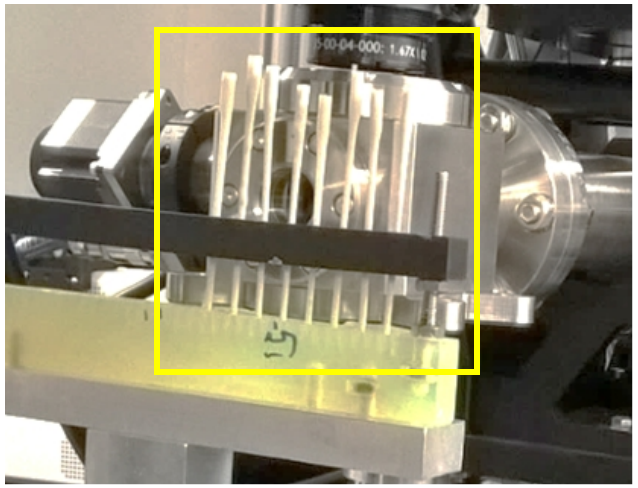

Fig. 3. Capillaries containing the fresh pastes mounted on the rack for synchrotron XRD data collection.

Fig. 4. Holder containing the fresh pastes, sandwiched between thin polyester films, for Cu Kα laboratory XRD data collection

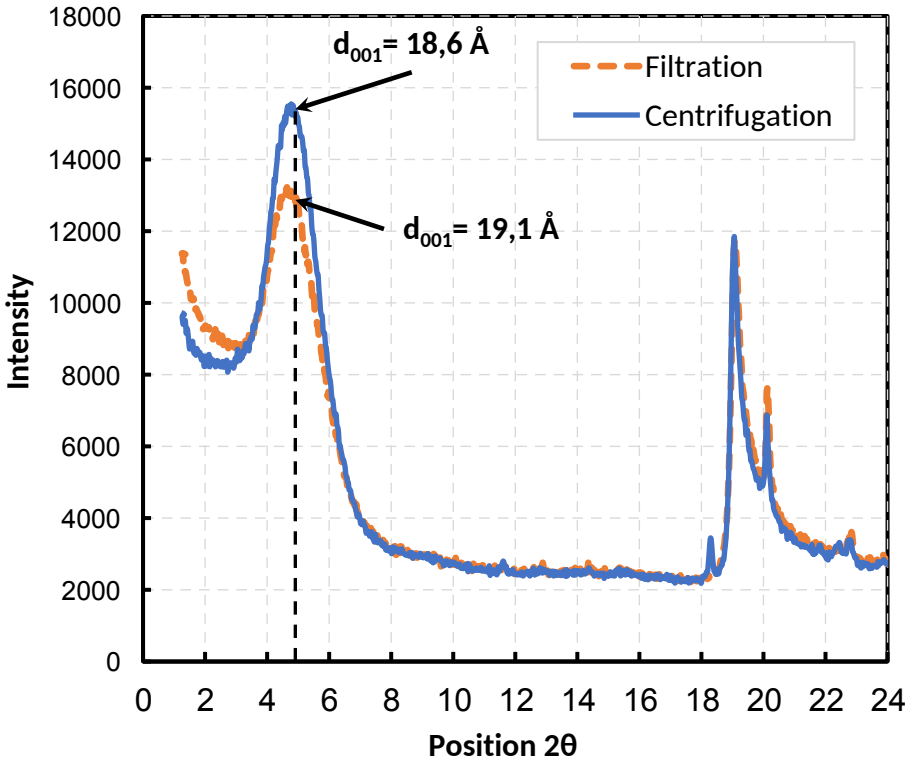

Fig. 5. Laboratory XRD patterns for dried clay pastes by using two different separation methods.

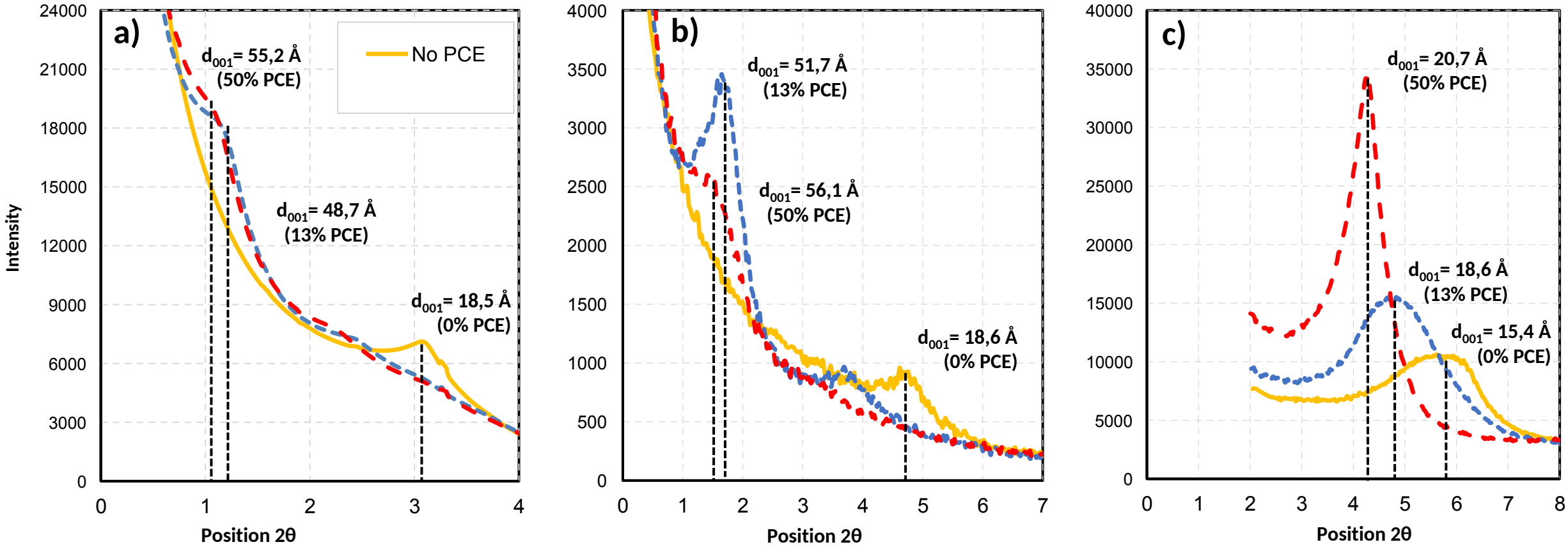

Fig. 6. XRD patterns for Na-MNT pastes with increasing PCE contents: a) data for fresh pastes collected with synchrotron radiation; b) data for fresh pastes collected with a Cu Kα diffractometer; c) data for centrifuged and dried pastes collected with a Cu Kα diffractometer.

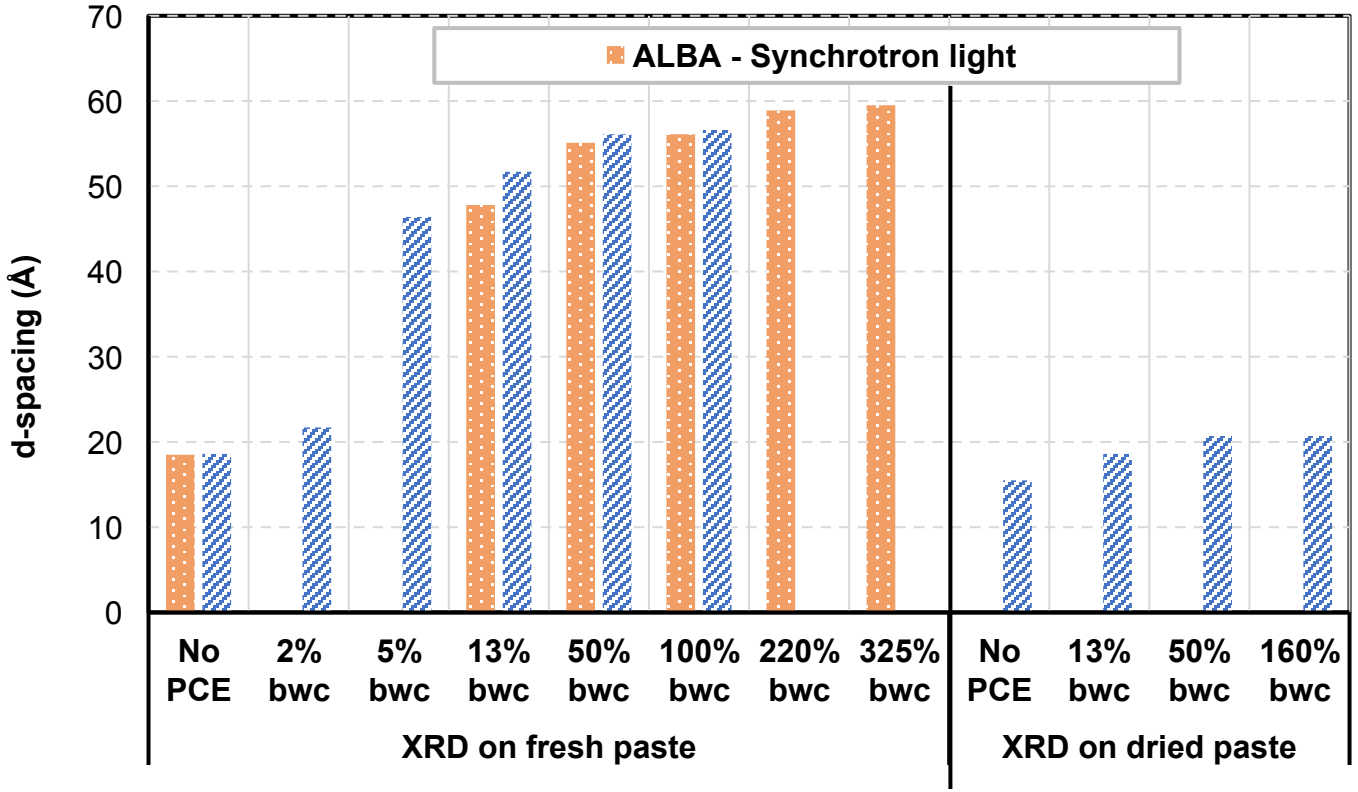

Fig.7. d-spacing of clay pastes with different PCE dosages and different XRD diffraction measurement conditions

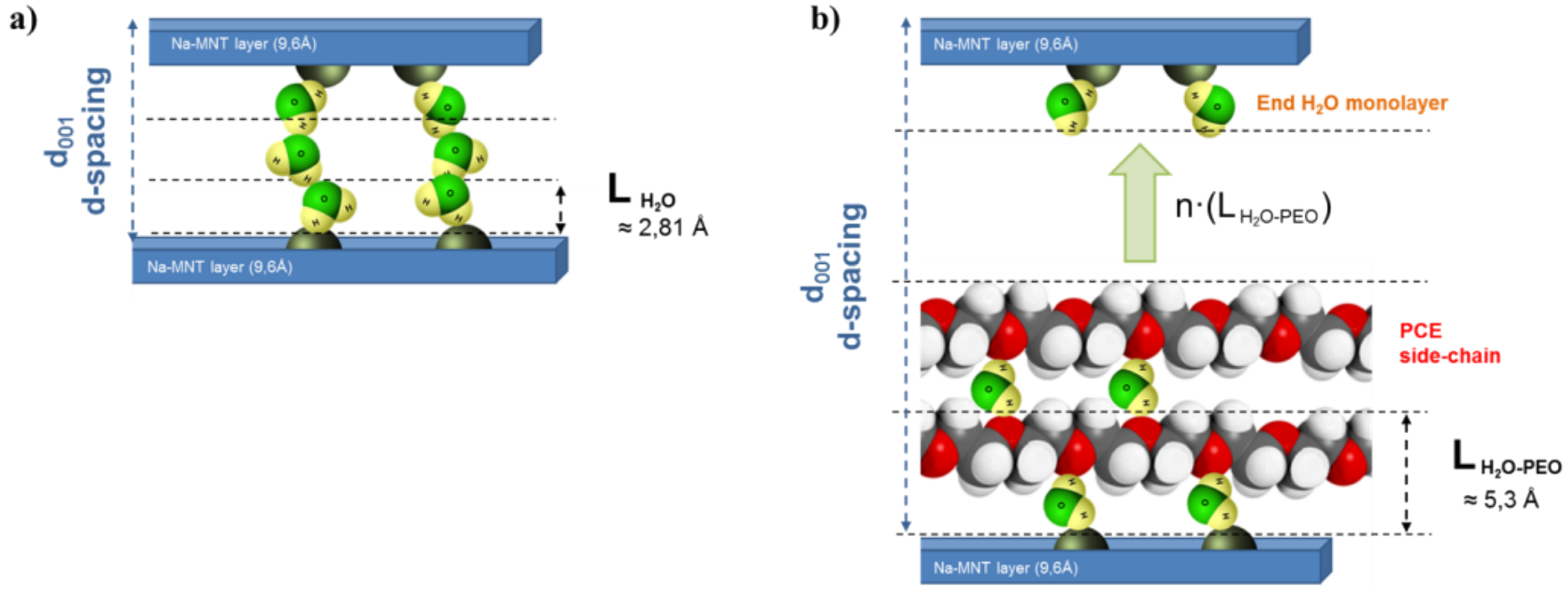

Fig.8. Intercalation models in MNT clay; a) without PCE polymer added; b) with PCE based admixture added